Conformation-Determined Through-Bond versus Through-Space Electronic Communication in Mixed-Valence Systems with a Cross-Conjugated Urea Bridge

ARTICLE *in* CHEMISTRY - A EUROPEAN JOURNAL · NOVEMBER 2014

Impact Factor: 5.73 · DOI: 10.1002/chem.201405332

3 AUTHORS, INCLUDING:

Zhong-Liang Gong
Chinese Academy of Sciences
16 PUBLICATIONS **160** CITATIONS

SEE PROFILE

ChemPubSoc Europe

DOI: 10.1002/chem.201405332

CHEMISTRY A European Journal Full Paper

Mixed-Valent Compounds

Conformation-Determined Through-Bond versus Through-Space Electronic Communication in Mixed-Valence Systems with a Cross-Conjugated Urea Bridge

Zhong-Liang Gong, Yu-Wu Zhong,* and Jiannian Yao[a]

Abstract: Bis-triarylamine **2** and cyclometalated diruthenium **6**$(PF_6)_2$ with a linear *trans*,*trans*-urea bridge have been prepared, together with the bis-triarylamine **3** and cyclometalated diruthenium **8**$(PF_6)_2$ with a folded *cis*,*cis*-*N*,*N*-dimethylurea bridge. The linear or folded conformations of these molecules are supported by single-crystal X-ray structures of **2**, **3**, and other related compounds. These compounds display two consecutive anodic redox waves ($N^{\bullet+/0}$ or $Ru^{III/II}$ processes) with a potential separation of 110–170 mV. This suggests that an efficient electronic coupling is present between two redox termini through the cross-conjugated urea bridge. The degree of electronic coupling has been investigated by using spectroelectrochemical measurements. Distinct intervalence charge-transfer (IVCT) transitions have been observed for mixed-valent (MV) compounds with a linear conformation. The IVCT transitions can also be identified for the folded MV compounds, albeit with a much weaker intensity. DFT results support that the electronic communication occurs by a through-bond and through-space pathway for the linear and folded compounds, respectively. The IVCT transitions of the MV compounds have been reproduced by TDDFT calculations. For the purpose of comparison, a bistriarylamine and a diruthenium complex with an imidazolidin-2-one bridge and a urea-containing mono-triarylamine and monoruthenium complex have been synthesized and studied.

Introduction

Electronic communications between redox active components are fundamental and crucial to the electron-transfer/transport processes occurring in nature and electronic devices.[1] In general, two kinds of processes, namely, through-bond and through-space communications are distinguished. The former relies on the orbital overlap between the redox termini and the bridging ligand.[2,3] The latter is a result of the charge sharing between/among closely spaced redox components.[4] Both processes can lead to the electrochemical potential splitting of redox sites and an intervalence charge-transfer (IVCT) transition in the near-infrared (NIR) region for the mixed-valent (MV) compounds.[2–4] Most MV compounds involve either through-bond or through-space coupling. It remains a challenge to realize both pathways in a single system.

The pioneering work of Creutz and Taube paved the way for the MV chemistry.[5] Since the proposal of using single molecules for the design of components for electronic devices, MV chemistry has received growing interest in various aspects of molecular electronics.[6] Important electronic-transfer parameters, such as reorganization energy and electronic coupling parameter, can be estimated by the IVCT analysis.[7]

To date, investigations of bridged MV systems have predominantly focused on π-conjugated systems and comparison with their saturated analogues. The uses of conjugated bridges are expected to strongly mediate the electronic communication between redox termini and thus be able to observe potential IVCT transitions for further analysis. Compared to linearly conjugated bridges, cross-conjugated compounds seem to be largely neglected in MV chemistry. A cross-conjugated compound possesses three unsaturated groups, two of which although conjugated to a third unsaturated center are not conjugated to each other.[8] Cross-conjugated molecules are well known,[9] and some representative examples are shown in the upper panel of Figure 1, including 1,1-diethynylalkene (A),[10] [3]dendralene (B),[11] and 1,1-diphenylalkene (C).[12] These components have been widely used in the design of molecular materials with optoelectronic functions.

Cross-conjugated bridges are normally inferior to their linearly conjugated counterparts in mediating charge delocalization. This is one reason why cross-conjugated bridge has received only little attention in MV chemistry and photoinduced electron-transfer processes. Wasielewski and Ratner reported that the photoinitiated charge separation through the cross-conjugated 1,1-diphenylethene bridge is about 30 times slower than through its linearly conjugated *trans*-stilbene counterpart.[13] Shultz and co-workers found that the MV quinone and semiquinone motif at the geminal positions of ethene (structure D in Figure 1) displayed efficient charge de-

[a] Z.-L. Gong, Prof. Dr. Y.-W. Zhong, Prof. Dr. J. Yao
Beijing National Laboratory for Molecular Sciences
CAS Key Laboratory of Photochemistry, Institute of Chemistry
Chinese Academy of Sciences, Beijing 100190 (China)
E-mail: zhongyuwu@iccas.ac.cn

Supporting information for this article is available on the WWW under http://dx.doi.org/10.1002/chem.201405332.

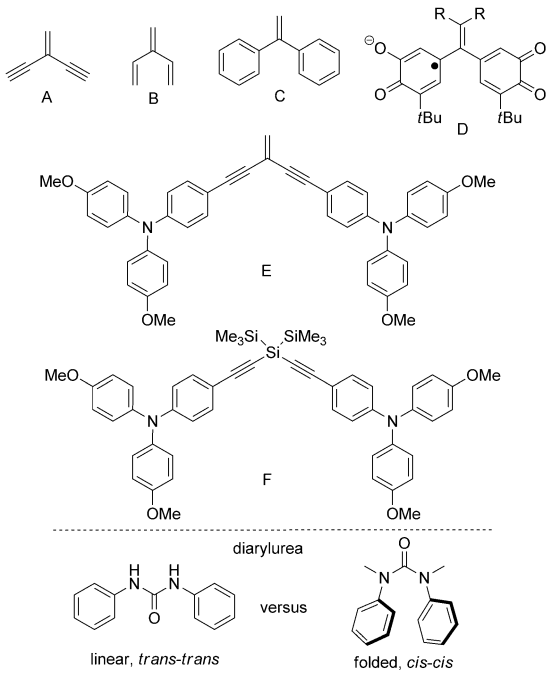

Figure 1. Cross-conjugated bridges and two typical conformations of diarylurea.

localization, as suggested by electrochemical potential splitting.[14] In addition, both electrochemical potential splitting and IVCT bands have been observed in porphyrin MV systems with a 1,1-diethenylalkene bridge.[15] Very recently, Hammarstrom and Ottosson and co-workers examined the electronic communication between two triarylamines through the cross-conjugated 1,1-diethynylalkene (Figure 1, E) and the cross-hyperconjugated 2,2-diethynyl-1,1,1,3,3,3-hexamethyltrisilane (Figure 1, F) bridge.[16] In addition to these advances, cross-conjugated molecules have recently received increased interest in single-molecule electronics with quantum interference effects, from both a theoretical and experimental perspective.[17]

We report herein on the first MV system with diarylurea as a cross-conjugated bridge. Depending on the substituents at the nitrogen atom, arylureas display significantly different conformations.[18] When the substituents are H atoms, diarylurea usually adopts a linear *trans*,*trans*-conformation (the bottom panel in Figure 1), and they are very important building blocks in supramolecular chemistry.[19] However, a simple *N*-methylation results in a folded *cis*,*cis*-conformation.[20] Such a folded face-to-face geometry has been used to connect photoactive donors and acceptors and realize charge-separation between them by Lewis and co-workers.[21] However, the use of diarylurea as a bridge in MV systems has not been explored,[22] either with a *trans*,*trans* or *cis*,*cis* conformation.

We considered that the well-defined linear and folded conformation of diarylurea can be utilized to switch the through-bond communication to the through-space coupling in MV systems. However, it is unknown whether the diarylurea is potent enough to mediate efficient electronic communication between redox termini, because diarylurea unit is a cross-conjugated molecule in nature. The two aryl groups are conjugated with the central carbonyl group; however, they are not conjugated to each other. We selected triarylamine and cyclometalated bistridentate ruthenium complex as the redox sites to build MV systems. Triarylamines have been widely used in organic MV compounds,[23] because they possess chemically reversible $N^{\bullet+/0}$ processes at low potentials and intense IVCT transitions. On the other hand, dicyclometalated ruthenium complexes, in which ruthenium ions are connected to the bridging ligand with a Ru–C bond, often show low $Ru^{III/II}$ potentials and strong metal–metal electronic communication.[24] We have prepared and studied the urea-bridged bistriarylamine compounds **2** and **3** and diruthenium complexes **6**$(PF_6)_2$ and **8**$(PF_6)_2$ (Scheme 1).

In addition, some other model compounds have been synthesized for comparison purpose (Scheme 2). These compounds were studied by combined experimental and computational methods, including single-crystal X-ray analysis, electrochemical and IVCT analysis, electron paramagnetic resonance (EPR) analysis, density functional theory (DFT), and time-dependent DFT (TDDFT) calculations.

Results and Discussion

Synthesis and single crystal X-ray analysis

Schemes 1 and 2 show the synthetic routes for compounds studied in this work. The reaction of N^1,N^1-di(*p*-anisyl)benzene-1,4-diamine (**1**)[25] with triphosgene in the presence of triethylamine gave an isocyanate intermediate, which was treated in situ with another equivalent of **1** to afford the urea-bridged bistriarylamine **2** in 84% yield. The double methylation of **2** using NaH/CH_3I gave the *N*,*N*′-dimethyl urea-bridged bistriarylamine **3** in 54% yield. By using the similar procedure for the synthesis of **2**, the bridging ligand **5** was obtained from the reaction of 3,5-di(pyrid-2-yl)aniline (**4**)[26] with triphosgene in 90% yield. Treatment of **4** with $[Ru(ttpy)Cl_3]$ (ttpy = 4′-tolyl-2,2′:6′,2″-terpyridine),[27] followed by anion exchange using KPF_6, gave the desired di-Ru complex **6**$(PF_6)_2$ in 23% yield. The dimethylation of **5** using NaH/CH_3I afforded the *N*,*N*′-dimethyl urea-bridged ligand **7** in 84% yield. The treatment of **7** with $[Ru(ttpy)Cl_3]$ or $[Ru(Me_3tctpy)Cl_3]$ (Me_3tctpy = trimethyl-4,4′,4″-tricarboxylate-2,2′:6′,2″-terpyridine)[28] gave complexes **8**$(PF_6)_2$ and **9**$(PF_6)_2$ in acceptable yield. Complex **9**$(PF_6)_2$ was synthesized for single-crystal X-ray analysis (see below).

Model compounds **11**, **12**, **15**$(PF_6)_2$, and **17**(PF_6) were prepared as outlined in Scheme 2. The Cu-catalyzed C–N coupling of *N*,*N*-di(*p*-anisyl)-4-iodoaniline (**10**)[29] with imidazolidin-2-one afforded compound **11** in 43% yield. In this compound, the urea unit is incorporated within an imidazolidin-2-one bridge and the conformation is locked to be linear. In addition, a urea-containing mono-triarylamine compound **12** was prepared from the treatment of **1** with triphosgene and *p*-toluidine.

Similarly, the Cu-catalyzed C–N coupling of 3,5-di(pyrid-2-yl)-bromobenzene (**13**)[30] with imidazolidin-2-one gave the bis-cyclometalating bridging ligand **14** in 48% yield. The reaction

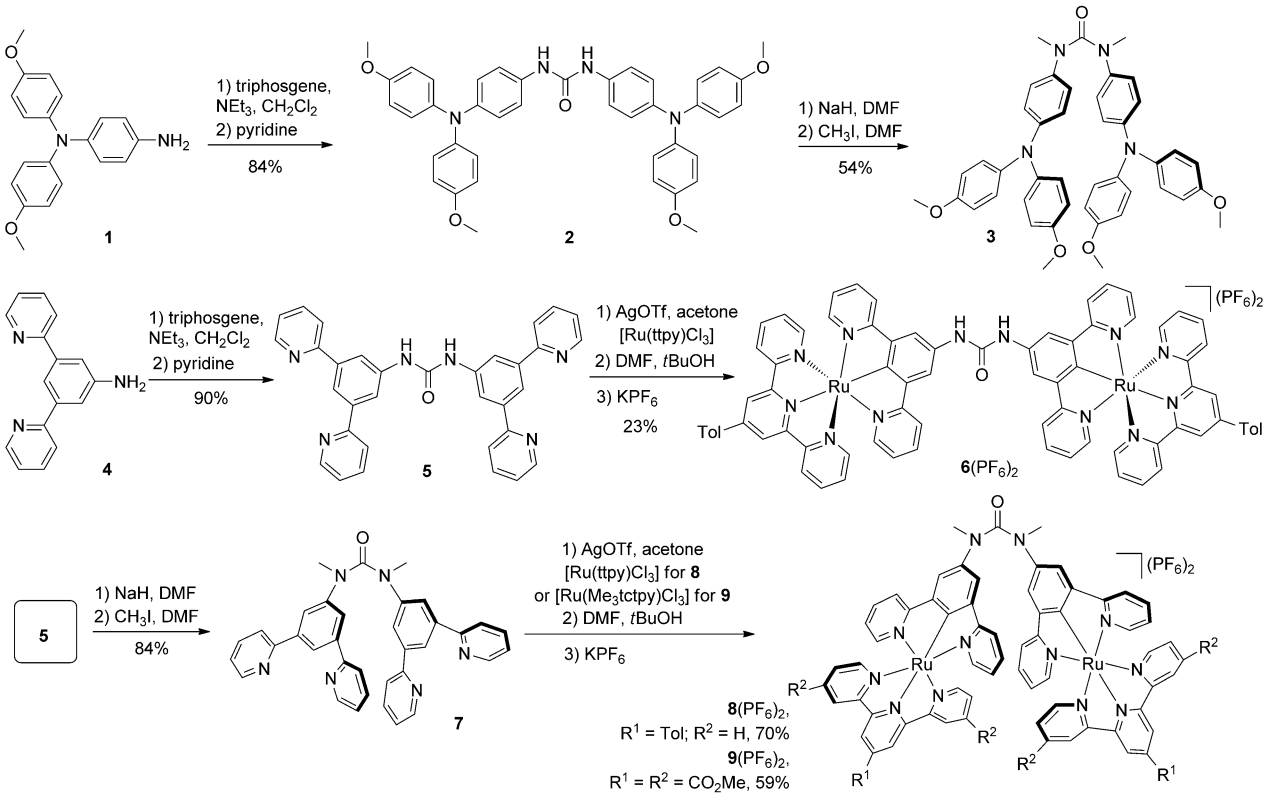

Scheme 1. Synthesis of urea-bridged compounds **2**, **3**, **6**$(PF_6)_2$, **8**$(PF_6)_2$, and **9**$(PF_6)_2$ (Tol is the *p*-tolyl group).

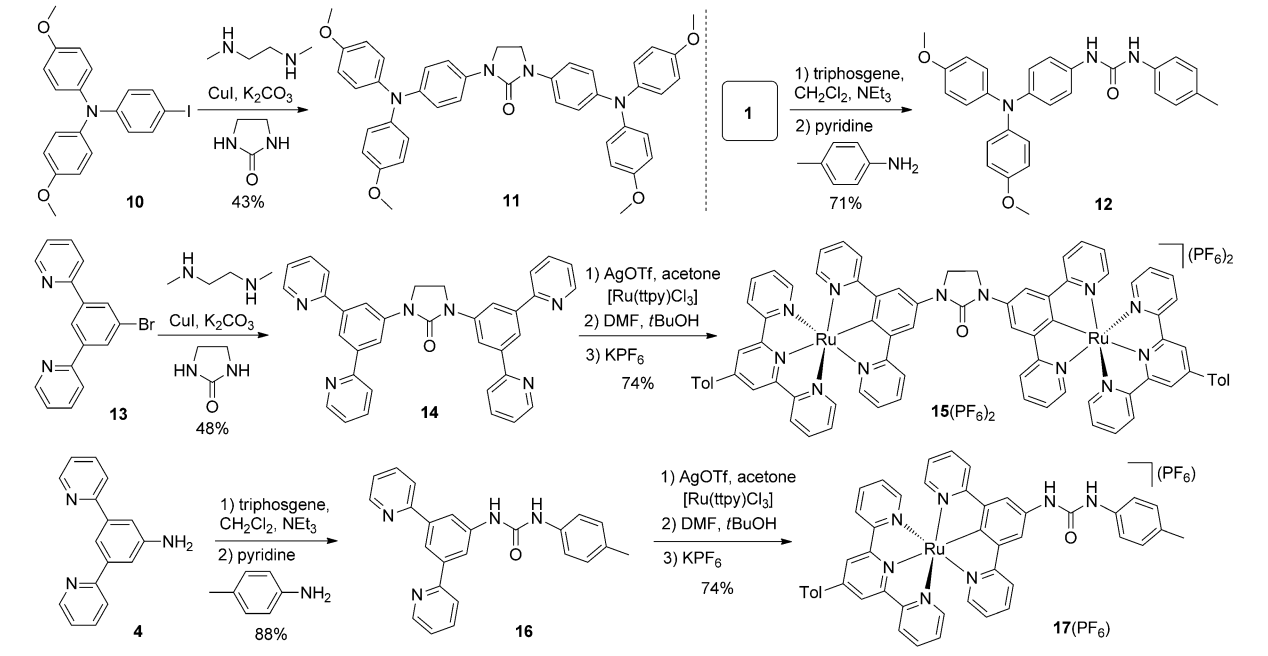

Scheme 2. Synthesis of model compounds **11**, **12**, **15**$(PF_6)_2$, and **17**(PF_6) (Tol is the *p*-tolyl group).

of **14** with $[Ru(ttpy)Cl_3]$, followed by anion exchange using KPF_6, provided the imidazolidin-2-one-bridged di-Ru complex **15**$(PF_6)_2$ in 74% yield. In addition, the treatment of **4** with triphosgene and *p*-toluidine afforded the urea-containing ligand **16**, which was treated with $[Ru(ttpy)Cl_3]$ to give the mono-Ru complex **17**(PF_6) in good yield. The synthesis and characterization of these compounds are depicted in the Experimental Section.

Single crystals of **2** have been obtained by diffusing petroleum ether into a solution in CH_2Cl_2. The X-ray structure shows

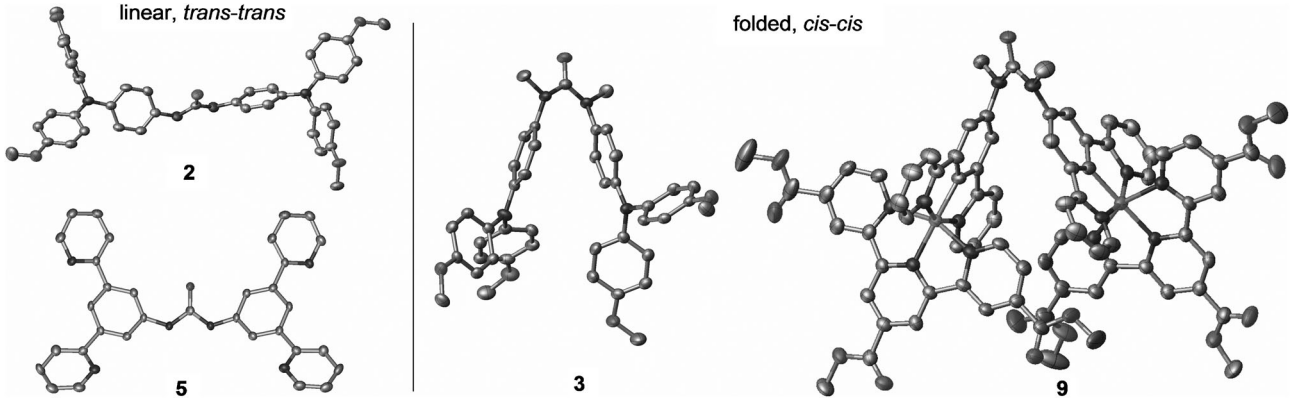

Figure 2. Thermal ellipsoid plots of the single-crystal X-ray structures of **2**, **3**, **5**, and **9**$(PF_6)_2$ at 30% probability. Hydrogen atoms and anions are omitted for clarity.

an expected linear conformation (left panel in Figure 2). The phenyl group directly connected to the urea unit has a torsion angle of 41.5° with respect to the urea plane. The triarylamine segment has a three-wheel propeller configuration. In the crystal packing, a typical urea-tape structure, assembled through intermolecular N–H···O hydrogen bonds, is observed (Supporting Information, Figure S1). In addition, single crystals of **3** have been obtained by diffusing *n*-hexane into a solution in 1,2-dichloroethane. The X-ray structure is shown in the right panel of Figure 2, which evidences a folded *cis*,*cis* conformation and face-to-face geometry of two triarylamines.

In comparison, it is much more difficult to obtain single crystals of di-Ru complexes. Up to date, we have failed to obtain a single crystal of complex **6**$(PF_6)_2$. However, a single crystal of the bridging ligand **5** was obtained by slow diffusion of hexane into a solution in CH_2Cl_2, and its X-ray crystallographic structure is shown in the left panel of Figure 2. This compound also has an expected linear *trans*,*trans* conformation. The phenyl groups directly connected to the urea unit are essentially co-planar with respect to the urea plane. No urea-tape structure can be discerned in the crystal packing, possibly inhibited by the steric hindrance of four pyridine groups. The reaction conditions used to transform **5** into the di-Ru complex **6**$(PF_6)_2$ are not believed to change the linear conformation.

We failed to obtain single crystals of the di-Ru complex **8**$(PF_6)_2$. Thus, complex **9**$(PF_6)_2$ with a different terminal ligand has been prepared. Fortunately, single crystals of **9**$(PF_6)_2$ were obtained by slow diffusion of hexane into a solution in CH_2Cl_2. The X-ray analysis shows that this complex has a folded *cis*,*cis* conformation, even with two bulky bistridentate ruthenium complexes. Each ruthenium ion has a distorted octahedral configuration and is connected to the bridging ligand with a Ru–C bond (1.98 Å in length). The two NCN-type cyclometalating ligands have a face-to-face geometry. The NNN terminal ligands are orthogonal to the cyclometalating ligand. The bite angle between two phenyl rings is 57° (Supporting Information, Figure S2). This angle is much bigger with respect to that of **3** (29°), apparently caused by the steric repulsion between two ruthenium components. Previous crystallographic studies show that this bite angle could be varied to a large degree (18–58°) depending on the substituents on the phenyl rings.[20] Complex **8**$(PF_6)_2$ is believed to have the similar folded conformation as **9**$(PF_6)_2$. They show similar electrochemical and spectroscopic properties as will be discussed below. The crystallographic data of **2**, **3**, **5**, and **9**$(PF_6)_2$ are summarized in Tables S1 and S2 in the Supporting Information.

Electrochemical studies

Electrochemical measurements are a useful means for probing the electronic communication in MV systems. In the case of zero coupling, a single two-electron redox wave is often observed. On the other hand, the observation of two separated one-electron redox waves indicates the presence of electronic coupling between two identical redox sites. However, care needs to be taken for this rule because electrochemical results are largely dependent on measurement conditions[31] and other factors, such as electrostatic repulsion and inductive effects, also contribute to the potential splitting.

Bistriarylamines **2**, **3**, and **11** all show two chemically reversible well-defined redox couples in the potential window between +0.2 and +1.0 V versus Ag/AgCl, as displayed in the cyclic voltammograms (CVs) and differential pulse voltammograms (DPVs) in Figure 3a and b. These signals are assigned to the stepwise oxidations of two triarylamine units in each compound ($N^{\bullet+/0}$ process).[23] In contrast, the monoamine compound **12** displays only one single redox couple within the same potential window. The potential splitting (ΔE) between two $N^{\bullet+/0}$ processes of **2**, **3**, and **11** is 130, 160, and 110 mV, respectively. This splitting is indicative of the amine–amine electronic communications between two triarylamine units in each compound. The comproportionation constant K_c for the equilibrium $[N^0–N^0]+[N^{\bullet+}–N^{\bullet+}]\rightarrow 2[N^0–N^{\bullet+}]$ is 160, 510, 70 for **2**, **3**, and **11**, respectively, as determined by $K_c = 10^{\Delta E/59(mV)}$ for a room-temperature case. This means that the MV states of these compounds have good thermodynamic stabilities. At the more positive region, some irreversible oxidation waves are observed for these compounds (Supporting Information, Figure S3), possibly caused by the further oxidation of the in situ-generated $N^{\bullet+}$ species ($N^{2+/\bullet+}$ process).[32]

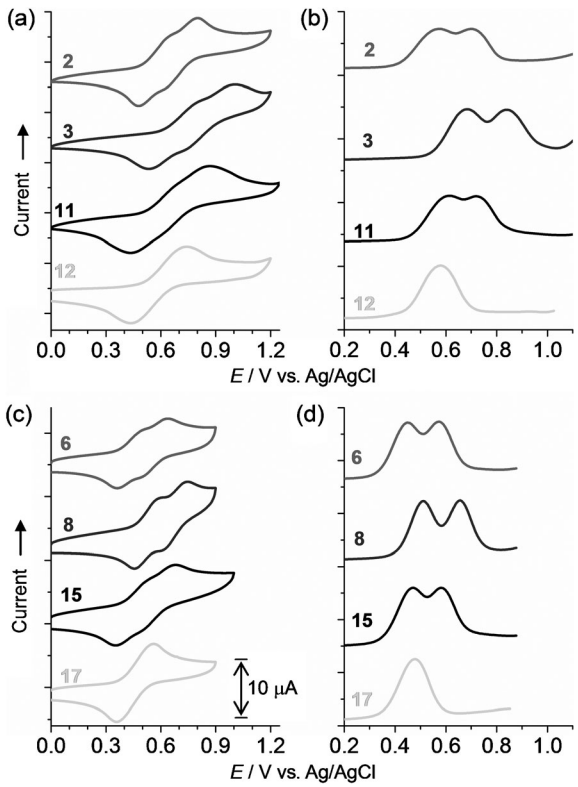

Figure 3. Anodic: a) CVs, and b) DPVs of triarylamine derivatives **2**, **3**, **11**, and **12**, and c) CVs, and d) DPVs of ruthenium complexes **6**$(PF_6)_2$, **8**$(PF_6)_2$, **15**$(PF_6)_2$, and **17**(PF_6) in 0.1 M Bu_4NClO_4/CH_2Cl_2. $E_{1/2} = +0.57$ and $+0.70$ V for **2**, $+0.68$ and $+0.84$ V for **3**, $+0.61$ and $+0.72$ V for **11**, $+0.58$ V for **12**, $+0.45$ and $+0.57$ V for **6**$(PF_6)_2$, $+0.51$ and $+0.65$ V for **8**$(PF_6)_2$, $+0.47$ and $+0.58$ V for **15**$(PF_6)_2$, and $+0.47$ V for **17**(PF_6).

As for the di-Ru complexes **6**$(PF_6)_2$, **8**$(PF_6)_2$, and **15**$(PF_6)_2$, two consecutive redox waves are observed in the similar potential window between $+0.2$ and $+1.0$ V versus Ag/AgCl (Figure 3c and d). These waves are mainly attributed to the $Ru^{III/II}$ processes. However, the involvement of the partial oxidation of the cyclometalating ligand is possible, because of the strong orbital overlap between the ruthenium ion and the electron-rich anionic phenyl ring. This is also the reason why the $Ru^{III/II}$ potential of cyclometalated ruthenium complexes is much lower with respect to noncyclometalated ruthenium complexes.[33] The potential splitting between two $Ru^{III/II}$ processes is 120, 140, and 110 mV for **6**$(PF_6)_2$, **8**$(PF_6)_2$, and **15**$(PF_6)_2$, respectively. The comproportionation constant K_c is 110, 240, and 70, respectively. The mono-Ru complex **17**(PF_6) shows one $Ru^{III/II}$ wave at $+0.47$ V in the same potential region. These results suggest that efficient electronic communication is also present between two ruthenium ions through the urea bridge.

Complex **9**$(PF_6)_2$ show similar two $Ru^{III/II}$ waves at $+0.66$ and $+0.83$ V; however, the potentials are slightly more positive relative to those of **8**$(PF_6)_2$ due to the electron-withdrawing nature of the Me_3tctpy ligand. At the more positive region, some additional oxidation waves are observed for all ruthenium complexes (Supporting Information, Figure S4). They are possibly caused by the $Ru^{IV/III}$ processes or ligand oxidation of cyclometalated ruthenium complexes.[24,33] In the negative scan, the ligand-based reduction waves can be observed. These data are of little relevance to the topic of this work and will not be discussed further. All of the above electrochemical data are summarized in the Supporting Information (Table S3).

Spectroscopic studies

To further probe the electronic coupling in these compounds, they were subjected to oxidative electrolysis at a transparent indium-tin-oxide (ITO) glass electrode. Figure 4 shows the absorption spectral changes of bis-triarylamines **2**, **3**, and **11** recorded during the spectroelectrochemical measurements. When the potential was gradually increased from $+0.40$ to $+0.65$ V versus Ag/AgCl to stepwise oxidize **2** (corresponding to the one-electron, single oxidation), an intense absorption band at 782 nm appeared (Figure 4a). This band is characteristic of the generation of the $N^{\bullet+}$ form (the $N^{\bullet+}$-localized transition).[23,32] Meanwhile, the appearance of a distinct absorption band between 1000 and 2500 nm was observed. When the potential was further increased to $+0.90$ V (corresponding to the second one-electron, double oxidation), the $N^{\bullet+}$-band continued to increase, but the NIR band gradually decreased until it disappeared completely (Figure 4b). This experiment clearly suggests that the observed NIR band of $\mathbf{2}^{\bullet+}$ belongs to the IVCT transition. Very similar absorption spectral changes have been observed during the single- and double-oxidation of **11** (Figure 4e and f) and a distinct IVCT band is evident for the MV state $\mathbf{11}^{\bullet+}$.

When the folded compound **3** was subjected to the single- and double oxidation, the increase of the $N^{\bullet+}$-localized transition was very clear in both (Figure 4c and d). It seems that no IVCT band can be assigned for the one-electron-oxidized form $\mathbf{3}^{\bullet+}$ at the first sight. However, a closer look at the enlarged plots in the NIR region clearly identifies a shoulder band around 1200 nm, which increases upon single oxidation and decreases upon double oxidation. This shoulder NIR band should be attributed to the IVCT transition, although it is much weaker with respect to those of $\mathbf{2}^{\bullet+}$ and $\mathbf{11}^{\bullet+}$.

Similar NIR absorption spectral changes have been observed when **6**$(PF_6)_2$, **8**$(PF_6)_2$, and **15**$(PF_6)_2$ were subjected to stepwise oxidations by electrolysis (Figure 5). For the linear di-Ru complexes **6**$(PF_6)_2$ and **15**$(PF_6)_2$, appreciably strong IVCT transitions have been observed in the NIR region, which increases upon single oxidation and decreases upon double oxidation. However, for the folded di-Ru complex **8**$(PF_6)_2$, only very weak IVCT transitions were identified in the MV state $\mathbf{8}^{3+}$ (Inset in Figure 5c and d). In addition to these changes, ruthenium complexes **6**$(PF_6)_2$, **8**$(PF_6)_2$, and **15**$(PF_6)_2$ show intense metal-to-ligand charge-transfer (MLCT) transitions in the visible region, which gradually decrease upon single and double oxidations. The new transitions around 700–800 nm are attributed to the ligand-to-metal charge-transfer (LMCT) transitions.[33] Complex **9**$(PF_6)_2$ show similar absorption spectral changes as **8**$(PF_6)_2$ (the Supporting Information, Figure S5), and weak IVCT transitions could be identified in the MV state.

Figure 6 shows the absorption spectral changes of the urea-containing mono-triarylamine **12** and mono-Ru complex

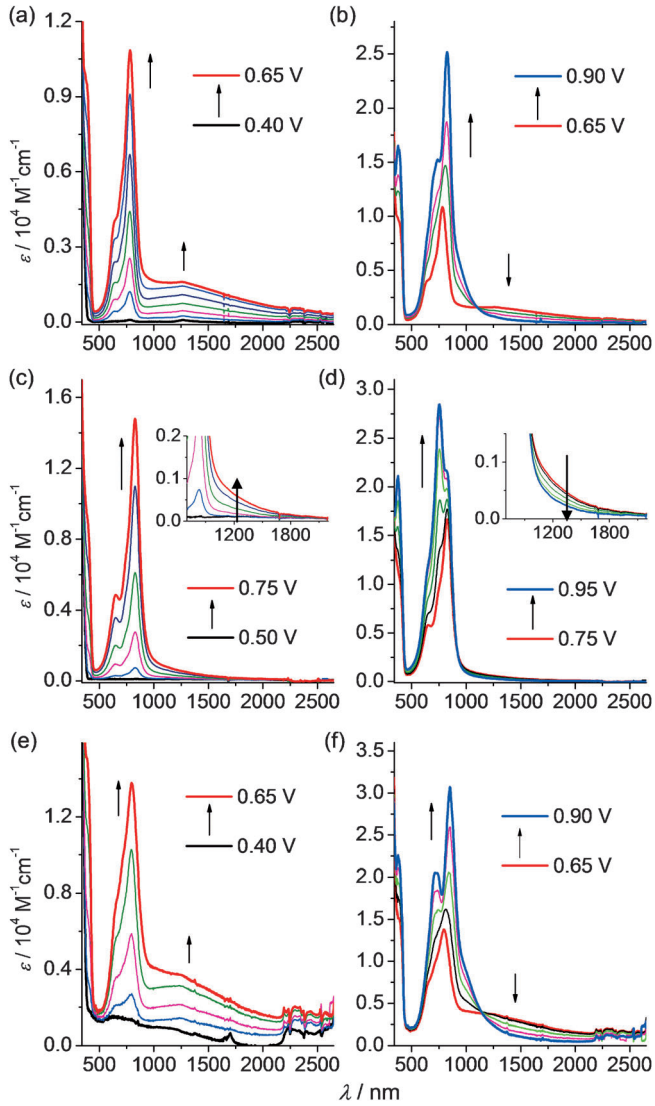

Figure 4. Absorption spectral changes of: a, b) **2**, c, d) **3**, and e, f) **11** in 0.1 M Bu_4NClO_4/CH_2Cl_2 by stepwise electrolysis using an ITO glass electrode. The applied potentials shown in the insets are referenced versus Ag/AgCl. a, c, e) One-electron oxidation; b, d, f) the second one-electron oxidation. The insets in (c, d) show the enlarged plots in the NIR region.

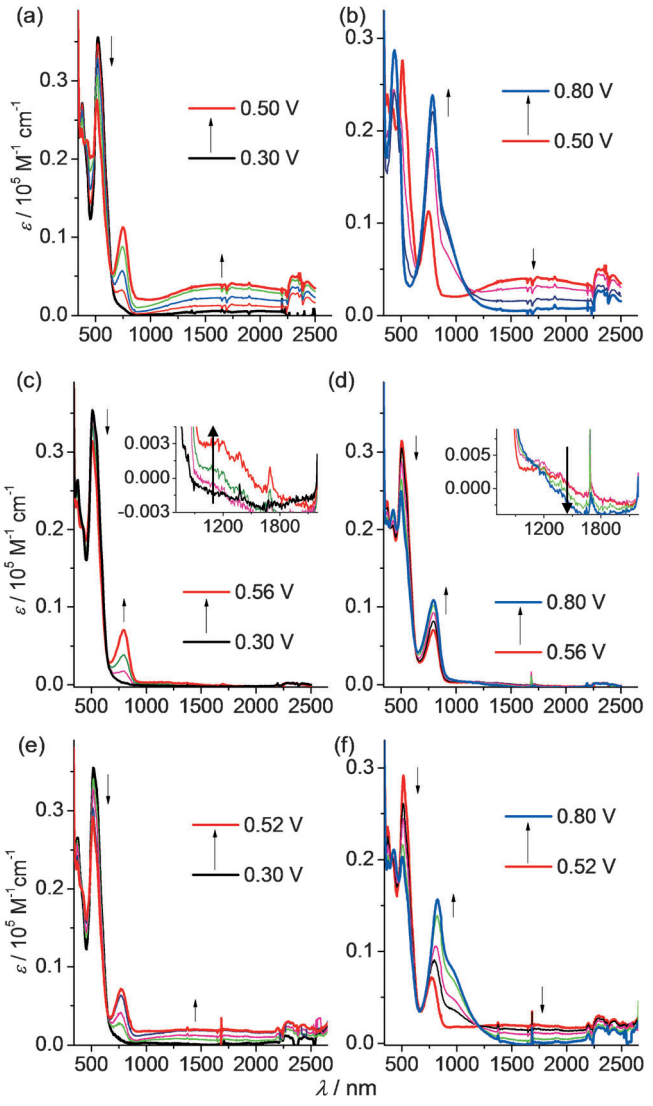

Figure 5. Absorption spectral changes of: a, b) **6**$(PF_6)_2$, c, d) **8**$(PF_6)_2$, and e, f) **15**$(PF_6)_2$ in 0.1 M Bu_4NClO_4/CH_2Cl_2 by stepwise electrolysis using an ITO glass electrode. The applied potentials shown in the insets are referenced versus Ag/AgCl. a, c, e) One-electron oxidation. b, d, f) the second one-electron oxidation. The insets in (c, d) show the enlarged plots in the NIR region.

17(PF_6) recorded during spectroelectrochemical measurements. Upon oxidation by electrolysis, the $N^{\bullet+}$-localized transition at 827 nm appeared for **12**. No NIR band has been observed. Similarly, the oxidation of **17**(PF_6) led to the decrease of the MLCT band at 519 nm and the appearance of the LMCT band at 784 nm. Again, no NIR band has appeared.

IVCT analysis and discussion on electronic communication

The above electrochemical and spectroscopic results strongly suggest that an efficient electronic communication is present between the redox termini through the cross-conjugated urea bridge. Since compounds **2**, **6**$(PF_6)_2$, **11**, and **15**$(PF_6)_2$ with the pristine urea bridge have a linear conformation, the electronic communication in these compounds is believed to be dominated by a through-bond mechanism. However, for the folded

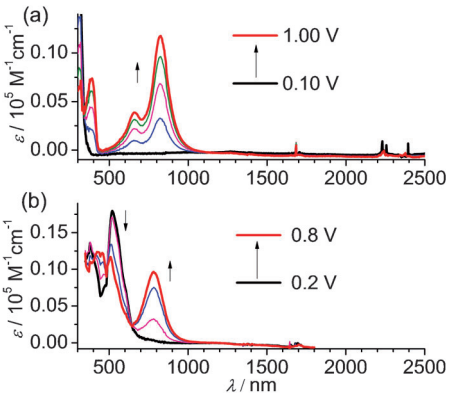

Figure 6. Absorption spectral changes of: a) **12**, and b) **17**(PF_6) by stepwise electrolysis using an ITO glass electrode versus Ag/AgCl.

compounds **3** and **8**$(PF_6)_2$ with the *N*,*N*-dimethyl diarylurea bridge, the redox sites, either triarylamine or cyclometalated ruthenium, have compact face-to-face conformation and a through-space coupling is believed to play an important role. It is impossible for the two ruthenium ions of **8**$(PF_6)_2$ to get into direct contact; however, it is known that there is high degree of charge delocalization between the ruthenium ion and the cyclometalating phenyl ring in cyclometalated ruthenium complexes[24,33] and a through-space coupling is thus possible through the orbital overlap between these two phenyl rings. This will be discussed further in the following DFT results.

To get more quantitative information on the electronic coupling, the NIR bands of $\mathbf{2}^{\bullet+}$, $\mathbf{3}^{\bullet+}$, $\mathbf{11}^{\bullet+}$, and $\mathbf{8}^{3+}$ were fitted to multiple symmetric curves using Gaussian functions (Figure 7). The fitted IVCT bands are highlighted in blue. The IVCT transitions of $\mathbf{6}^{3+}$ and $\mathbf{15}^{3+}$ are well separated from the LMCT transitions in the visible region and thus are directly used for the following analysis.

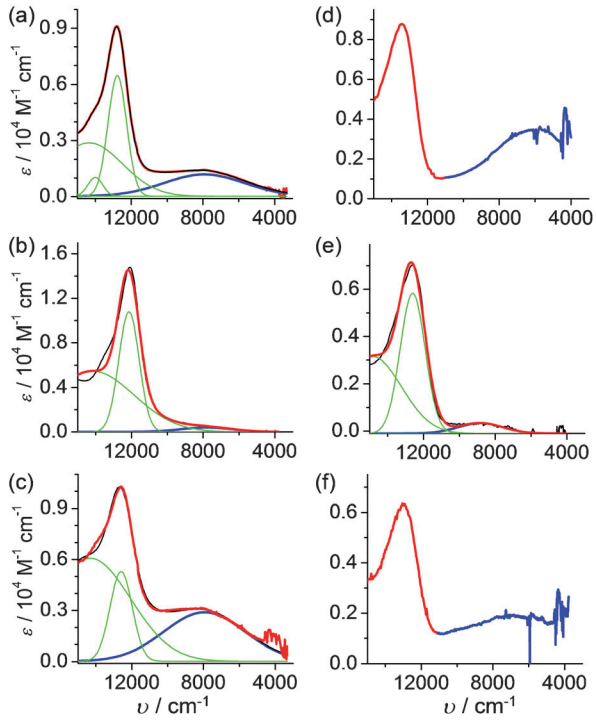

Figure 7. NIR absorptions (red curves) and IVCT transitions (blue curves) of: a) $\mathbf{2}^{\bullet+}$, b) $\mathbf{3}^{\bullet+}$, c) $\mathbf{11}^{\bullet+}$, d) $\mathbf{6}^{3+}$, e) $\mathbf{8}^{3+}$, and f) $\mathbf{15}^{3+}$ as a function of wavenumbers. The IVCT bands in (a, b, c, e) were obtained by Gaussian deconvolution.

The IVCT parameters are summarized in Table 1. The linear compounds have much more intense IVCT bands with respect to those of the folded compounds. The bandwidths at half height ($\Delta\nu_{1/2,obs}$) of all IVCT bands, except $\mathbf{3}^{\bullet+}$ and $\mathbf{8}^{3+}$ with very weak ones, are slightly broader, but of the same order of magnitude, with respect to the theoretical value ($\Delta\nu_{1/2,theo}$) for a Robin–Day class II system.[34] The electronic coupling parameter V_{ab} is determined to be 390, 310, 540, 480, 240, and 480 cm^{-1} for $\mathbf{2}^{\bullet+}$, $\mathbf{3}^{\bullet+}$, $\mathbf{11}^{\bullet+}$, $\mathbf{6}^{3+}$, $\mathbf{8}^{3+}$, and $\mathbf{15}^{3+}$, respectively, by the Hush formula,[6] $V_{ab} = 0.0206(\varepsilon_{max}\nu_{max}\Delta\nu_{1/2})^{1/2}/(r_{ab})$. The electron-transfer distance r_{ab} is estimated by the DFT-calculated geometrical distance between two distal nitrogen or ruthenium atoms. The folded compounds $\mathbf{3}^{\bullet+}$ and $\mathbf{8}^{3+}$ have smaller V_{ab} values with respect to other four linear compounds, although the folded compounds have much smaller r_{ab} values. The V_{ab} values of the linear bistriarylamines $\mathbf{2}^{\bullet+}$ and $\mathbf{11}^{\bullet+}$ are smaller than, but comparable to that of 4,4′-bis(*N*,*N*-di-*p*-anisylamino)tolane with a conjugated bridge yet comparable N–N distance ($r_{ab} = 12.48$ Å; $V_{ab} = 3.1$ kcal $mol^{-1} = 1080$ cm^{-1}).[35] In addition, the linear di-Ru complexes $\mathbf{6}^{3+}$ and $\mathbf{15}^{3+}$ have a comparable V_{ab} value with respect to a cyclometalated di-Ru complex with a conjugated tolane bridge ($r_{ab} = 13.7$ Å; $V_{ab} = 0.070$ eV $= 565$ cm^{-1}).[36] This suggests that the non-conjugated urea is indeed a potent bridge to mediate electronic coupling.

Table 1. IVCT parameters.

	$\mathbf{2}^{\bullet+}$	$\mathbf{3}^{\bullet+}$	$\mathbf{11}^{\bullet+}$	$\mathbf{6}^{3+}$	$\mathbf{8}^{3+}$	$\mathbf{15}^{3+}$
λ_{max} [nm]	1250	1280	1260	1680	1140	1430
ν_{max} [cm^{-1}]	8000	7800	7950	6000	8800	7000
ε_{max} [$M^{-1}cm^{-1}$]	1500	390	2800	3500	330	2000
$\Delta\nu_{1/2,obs}$[a] [cm^{-1}]	5340	3310	5400	5200	3000	7600
$\Delta\nu_{1/2,theo}$[a] [cm^{-1}]	4300	4240	4285	3720	4500	4020
r_{ab}[b] [Å]	13.24	6.61	13.11	14.28	8.05	14.06
V_{ab}[c] [cm^{-1}]	390	310	540	480	240	480

[a] Full width at half height, calculated by $\Delta\nu_{1/2,theo} = (2310\,\nu_{max})^{1/2}$. [b] DFT-optimized N–N or Ru–Ru geometrical distance. [c] Calculated by using the Hush formula.

In addition, both the pristine urea and imidazolidin-2-one unit are efficient in mediating the electronic coupling, suggesting that the intermolecular H-bonds in the urea-tape structure of **2** are not decisive in the underlying electron-transfer process. It should be also mentioned that the positive charge of the above MV systems is rather delocalized and the true r_{ab} is expected to be shorter than the geometrical distance.

EPR studies

MV bistriarylamines $\mathbf{2}^{\bullet+}$, $\mathbf{3}^{\bullet+}$, and $\mathbf{11}^{\bullet+}$, obtained by chemical oxidation using $SbCl_5$ in CH_2Cl_2, all show a single-line EPR peak at $g = 2.006$ at room temperature (Figure 8). In the doubly oxidized state, the linear compounds $\mathbf{2}^{2+}$ and $\mathbf{11}^{2+}$ show slightly broad yet comparably intense EPR signal with respect to their singly oxidized states. However, the EPR intensity of the folded bistriarylamine $\mathbf{3}^{2+}$ doubled relative to that of its singly oxidized form, $\mathbf{3}^{\bullet+}$. This suggests that $\mathbf{3}^{2+}$ is a purely triplet diradical ($S = 1$) and potentially useful as organic high-spin materials.[37] For the linear compounds $\mathbf{2}^{2+}$ and $\mathbf{11}^{2+}$, both triplet and open-shell singlet diradical could co-exist; however, the triplet state may account for a higher proportion. Because of the presence of the cross-conjugated bridge, a closed-shell singlet form cannot exist for these doubly charged compounds. Note that among these three states, only the triplet state is EPR active.[38]

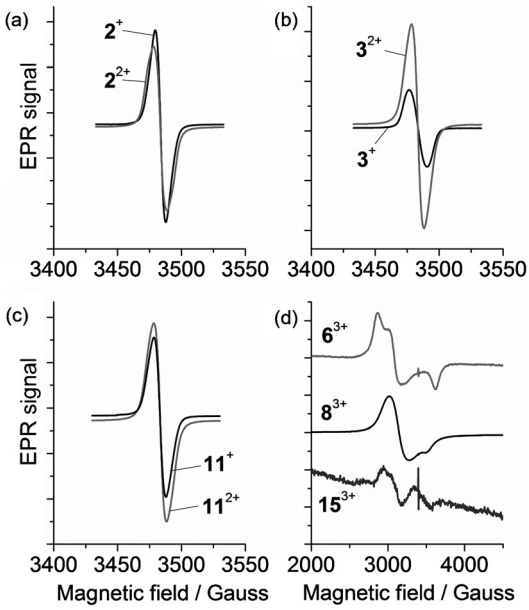

Figure 8. EPR signals of: a) $\mathbf{2}^{\bullet+}$ and $\mathbf{2}^{2+}$, b) $\mathbf{3}^{\bullet+}$ and $\mathbf{3}^{2+}$, c) $\mathbf{11}^{\bullet+}$ and $\mathbf{11}^{2+}$ in CH_2Cl_2 at room temperature, and d) $\mathbf{6}^{3+}$, $\mathbf{8}^{3+}$, and $\mathbf{15}^{3+}$ in CH_3CN at 77 K.

MV di-Ru complexes $\mathbf{6}^{3+}$, $\mathbf{8}^{3+}$, and $\mathbf{15}^{3+}$, obtained by chemical oxidation using cerium ammonium nitrate in CH_3CN, are EPR silent at room temperature. However, they show a distinct rhombic ($\mathbf{6}^{3+}$ and $\mathbf{15}^{3+}$) or axial ($\mathbf{8}^{3+}$) EPR signal at 77 K in frozen CH_3CN. For complex $\mathbf{6}^{3+}$, the electron g factor g_1, g_2, and g_3 value is 2.367, 2.200, and 1.875, respectively. The anisotropy Δg ($=g_1-g_3$) is 0.492 and the isotropic g factor $<g>$ ($=[(g_1^2+g_2^2+g_3^2)/3]^{1/2}$) is 2.157. For complex $\mathbf{8}^{3+}$, $g_1=g_2=$ 2.170 and $g_3=1.951$. The isotropic g factor $<g>$ of $\mathbf{8}^{3+}$ is 2.099. For complex $\mathbf{15}^{3+}$, the g_1, g_2, g_3, and $<g>$ value is 2.311, 2.192, 1.904, and 2.142, respectively. It has been reported that a true metal-centered spin of a cetecholatoruthenium(III) complex has a $<g>$ value of 2.476 with $\Delta g=0.833$.[39] The relatively low $<g>$ value of $\mathbf{6}^{3+}$, $\mathbf{8}^{3+}$, and $\mathbf{15}^{3+}$ may be caused by the spin delocalization between the ruthenium ion and the cyclometalating phenyl ring. Such EPR characteristics have previously been observed in MV systems with cyclometalated ruthenium complexes.[24] The doubly oxidized forms of these complexes are EPR silent even at low temperature. This is likely caused by the fast spin relaxation of ruthenium ions.

DFT and TDDFT studies

DFT calculations have been performed on the urea-bridged bis-triarylamines **2**, **3**, and **11** and di-Ru complexes $\mathbf{6}^{2+}$, $\mathbf{8}^{2+}$, and $\mathbf{15}^{2+}$ on the Gaussian 09 package.[40] The hybrid B3LYP exchange correlation functional[41] with the LANL2DZ basis set[42] for Ru and 6-31G* for other atoms[43] were used. The computations were carried out taking into account solvation effects in CH_2Cl_2 solution.

The DFT-calculated frontier molecular orbital energy orderings of the above compounds are shown in Figure S6 in the Supporting Information. Figure 9 shows the isodensity plots of the highest occupied molecular orbital (HOMO), HOMO−1, and the lowest unoccupied molecular orbital (LUMO) of three bis-triarylamines. All of these orbitals are dominated by the triarylamine units. The bridging urea unit of the linear compounds **2** and **11** makes appreciable contributions to these orbitals, which suggests that the electronic communication occurs through a through-bridge (or through-bond) pathway. In contrast, the electron density on the urea unit of the folded compound **3** is negligible, suggesting that the through-bond mechanism is unfavorable. On the other hand, the LUMO and HOMO-1 orbitals of **3** show direct p-orbital overlap between the two phenyl rings connected to the urea unit (highlighted by red circles in Figure 9). This supports that the electron communication between two triarylamine units in the folded compound **3** very likely occurs by a through-space mechanism.

The isodensity plots of the frontier molecular orbitals of the di-Ru complexes $\mathbf{6}^{2+}$, $\mathbf{8}^{2+}$, and $\mathbf{15}^{2+}$ are given in Figures S7–S9 in the Supporting Information. The low-energy unoccupied orbitals (from LUMO to LUMO+3) of these complexes are dominated by the terminal ligands. The LUMO+4 has major contribution from the cyclometalating ligand. The HOMO and HOMO-1 of all complexes are dominated by the Ru-phenyl components, reflecting the charge delocalization of cyclometalated ruthenium complexes. In addition, the bridging urea unit of the linear complexes $\mathbf{6}^{2+}$ and $\mathbf{15}^{2+}$ makes some contribu-

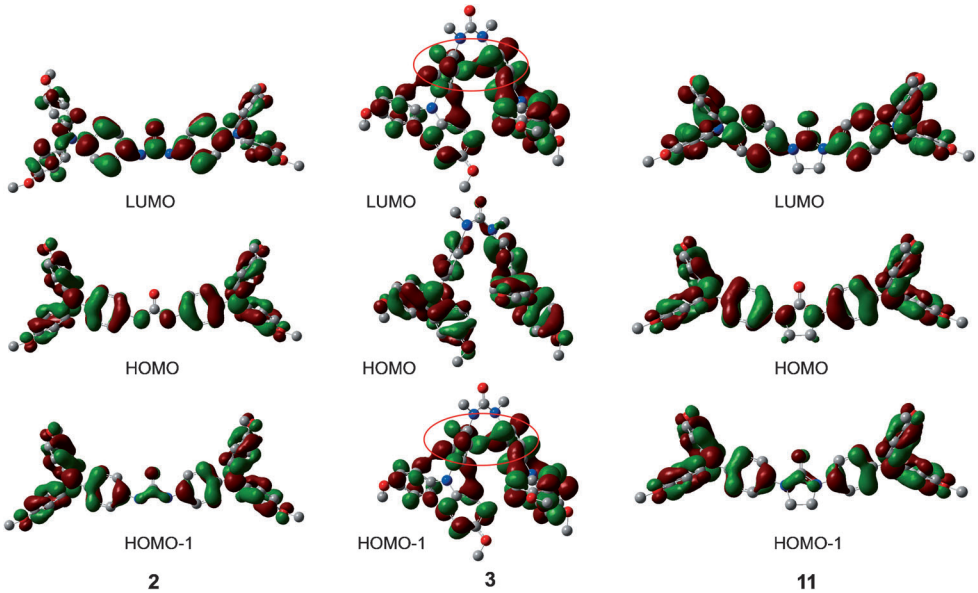

Figure 9. Frontier molecular orbitals of **2**, **3**, and **11**. The red circles highlight the through-space orbital overlap between two phenyl rings separated by the urea bridge.

tions to the HOMO and HOMO−1 orbitals, supporting a through-bond mechanism. Moreover, a HOMO-mediated hole-transfer tunneling, versus electron-transfer tunneling, is more likely the dominating pathway as has been discussed in MV complexes with cyclometalated ruthenium complexes.[24,28] For the folded di-Ru complex $\mathbf{8}^{2+}$, the HOMO−1 and LUMO+4 orbitals show direct p-orbital overlap between the two phenyl rings connected to the urea unit (Supporting Information, Figure S8), again supporting a through-space electron-sharing pathway.

Based on above optimized structures, DFT calculations have been performed on the doublet singly oxidized forms and triplet doubly oxidized forms, using the same level of theory. The calculated Mulliken spin density distributions are shown in the Supporting Information, Figure S10. The free spin of the linear bistriarylamines $\mathbf{2}^{+}$ and $\mathbf{11}^{+}$ is delocalized on both triarylamine components. However, the spin density distribution of the linear di-Ru complexes $\mathbf{6}^{3+}$ and $\mathbf{15}^{3+}$ is clearly asymmetric. For the folded compounds $\mathbf{3}^{+}$ and $\mathbf{8}^{3+}$, the free spin is localized on one triarylamine or ruthenium component. This is consistent with the above IVCT analysis, which shows that the folded compounds have a smaller electronic coupling with respect to the linear compounds. In the triplet doubly oxidized states, the spins are dominated by both redox sites, regardless of the conformation of the molecule. However, these results should be taken with care because DFT calculations are known to overestimate charge delocalization and the results are largely dependent on the calculation methods.[44]

The IVCT transitions of the MV bis-triarylamine compounds $\mathbf{2}^{\bullet+}$, $\mathbf{3}^{\bullet+}$, $\mathbf{11}^{\bullet+}$ and di-Ru complexes $\mathbf{6}^{3+}$, $\mathbf{8}^{3+}$, and $\mathbf{15}^{3+}$ can be predicted by the TDDFT calculations (Supporting Information, Table S4 and Figures S11 and S12). The predicted D_1 excitations (D = doublet) of these open-shell compounds have the dominant spin transitions from the β-highest occupied spin orbital (HOSO) to the β-lowest unoccupied spin orbital (LUSO), which are attributable to the IVCT transitions. The linear compounds $\mathbf{2}^{\bullet+}$, $\mathbf{11}^{\bullet+}$, $\mathbf{6}^{3+}$, and $\mathbf{15}^{3+}$ are predicted to have IVCT transitions with high oscillator strengths (f = 0.5534, 0.5927, 0.4744, 0.4182, respectively). On the other hand, the folded compounds $\mathbf{3}^{\bullet+}$ and $\mathbf{8}^{3+}$ are predicted to have very weak IVCT transitions with an oscillator strength of 0.0031 and 0.0106, respectively. This trend agrees well with the above experimental results, in which the linear MV compounds show much more intense IVCT transitions with respect to the folded compounds. One discrepancy is that the predicted IVCT transitions are all lower in energy relative to the observed ones, which reflects the limitation of TDDFT computations for open-shell compounds. At higher energies, the $N^{\bullet+}$-localized transitions for the bis-triarylamine compounds (D_4 of $\mathbf{2}^{+}$, D_2 of $\mathbf{3}^{+}$, and D_3 of $\mathbf{11}^{+}$) and the LMCT transitions for the di-Ru compounds (D_6 of $\mathbf{6}^{3+}$, $\mathbf{8}^{3+}$, and $\mathbf{15}^{3+}$) have been reproduced.

Conclusion

We have demonstrated in this work the first MV system with a cross-conjugated urea bridge. The linear diarylurea has been found to be an efficient bridge to mediate the electronic communication between two organic or inorganic redox termini. More importantly, the strength of the cross-conjugated diarylurea in mediating the electron coupling is comparable to the conjugated bridge (e.g., tolane) of similar length. This information is of great significance for the design of new MV systems and other organic and organometallic materials for molecular electronics. Previous studies have shown that the charge-transfer bands of donor–acceptor compounds with a cross-conjugated bridge are very weak and even indiscernible.[9,10,13,45] The urea unit represents a rare cross-conjugated bridge that can give rise to distinct IVCT transitions (ε_{max} up to 3500 $M^{-1}cm^{-1}$) in MV systems with a medium distance between redox termini (up to 14 Å). In addition, the urea unit has been very useful in supramolecular chemistry to build stimuli-responsive materials.[19] The use of urea bridge in MV chemistry will allow us to make new supramolecular materials with charge-transfer functions.

By virtue of the substituent-dependent conformation of urea, the through-bond electronic coupling in linear molecules is switched to the through-space communication in folded *N*,*N*-dimethyl diarylurea molecules. The through-space coupling in folded molecules is supported by single-crystal X-ray structures and DFT results. Interestingly, the folded conformation persists even with two sterically demanding hexacoordinated ruthenium complexes, which suggests the general applicability of this chemistry.

Experimental Section

Spectroscopic measurements

Absorption spectra were recorded on a PE Lambda 750 UV/Vis/NIR spectrophotometer at room temperature. Spectroelectrochemical measurements were performed in a thin layer cell (optical length = 0.2 cm), in which an ITO glass electrode (< 10 Ω square^{-1}) working electrode was set in the indicated solvent containing the compound to be studied (concentration around 5×10^{-5} M) and 0.1 M Bu_4NClO_4 as the supporting electrolyte. A platinum wire and Ag/AgCl in saturated aqueous NaCl was used as the counter electrode and reference electrode, respectively. The cell was put into the spectrometer to monitor the spectral change during electrolysis.

Electrochemical measurements

All electrochemical measurements were taken using a CHI 660D potentiostat with one-compartment electrochemical cell under an atmosphere of nitrogen. All measurements were carried out in 0.1 M Bu_4NClO_4 in indicated solvents at a scan rate of 100 mV s^{-1}. The working electrode was a glassy carbon with a diameter of 3 mm. The electrode was polished prior to use with 0.05 μm alumina and rinsed thoroughly with water and acetone. A large area platinum wire coil was used as the counter electrode. All potentials are referenced to an Ag/AgCl electrode in saturated aqueous NaCl without regard for the liquid junction potential. The potential versus ferrocene$^{+/0}$ can be subtracted by 0.45 V.

X-ray crystallography

The X-ray diffraction data were collected using a Rigaku Saturn 724 diffractometer on a rotating anode ($Mo_{K\alpha}$ radiation, 0.71073 Å) at

173 K. The structure was solved by the direct method using SHELXS-97[46] and refined with Olex2.[47]

Computational methods

DFT calculations are carried out using the B3LYP exchange correlation functional[41] and implemented in the Gaussian 09 package.[40] The electronic structures were optimized using a general basis set with the Los Alamos effective core potential LanL2DZ basis set for Ru[42] and 6-31G* for other atoms.[43] The solvation effects in dichloromethane solutions are taken into account for all calculations. No symmetry constraints were used in the optimization (nosymm keyword was used). Frequency calculations have been performed with the same level of theory to ensure the optimized geometries to be local minima. All orbitals have been computed at an isovalue of 0.02 e bohr^{-3}.

EPR measurements

EPR measurements were performed on a Bruker ELEXSYS E500-10/12 spectrometer at room temperature in CH_2Cl_2 solutions for triarylamine derivatives or at frozen CH_3CN for ruthenium complexes. The spectrometer frequency is 9.7×10^9 Hz.

Syntheses

General procedures

NMR spectra were recorded in the designated solvent on Bruker Avance 400 MHz spectrometer. Spectra are reported in ppm values from residual protons of deuterated solvent. Mass data were obtained with a Bruker Daltonics Inc. Apex II FT-ICR or Autoflex III MALDI-TOF mass spectrometer. The matrix for MALDI-TOF measurement is α-cyano-4-hydroxycinnamic acid. Microanalysis was carried out using Flash EA 1112 or Carlo Erba 1106 analyzer at the Institute of Chemistry, Chinese Academy of Sciences. N^1,N^1-Di(*p*-anisyl)benzene-1,4-diamine (**1**),[25] 3,5-di(pyridin-2-yl)aniline (**4**),[26] *N*,*N*-di(*p*-anisyl)-4-iodoaniline (**10**),[29] and 3,5-di(pyrid-2-yl)bromobenzene (**13**)[30] were prepared according to known procedures.

Synthesis of 2

A mixture of triphosgene (125 mg, 0.42 mmol) and triethylamine (0.5 mL) in dichloromethane (5 mL) was cooled to 0 °C in the ice bath, followed by the addition of N^1,N^1-di(*p*-anisyl)benzene-1,4-diamine (135 mg, 0.42 mmol). One hour later, another bath of N^1,N^1-di(*p*-anisyl)benzene-1,4-diamine (128 mg, 0.40 mmol) in pyridine (5 mL) was added. The resulting solution was heated at 95 °C for 2 h. The system was cooled to room temperature and the solvent was removed under vacuum. This crude product was purified by column chromatography on silica gel (eluent: CH_2Cl_2/C_2H_5OH, 25:1) to give **2** (223 mg) as a pale-yellow solid in 84% yield. ^{1}H NMR (400 MHz, [D$_6$]acetone): $\delta=3.76$ (s, 12H), 6.86 (d, $J=8.0$ Hz, 12H), 6.96 (d, $J=7.6$ Hz, 8H), 7.38 (d, $J=8.0$ Hz, 4H), 7.95 ppm (s, 2H); ^{13}C NMR (100 MHz, [D$_6$]DMSO): $\delta=55.19$, 114.75, 119.48, 122.67, 124.95, 133.95, 141.03, 142.54, 152.60, 154.82 ppm; MALDI-TOF (*m/z*): 666.3 for $[M]^+$; ESI-HRMS: *m/z* calcd for $C_{41}H_{38}N_4O_5$: 666.2824; found: 666.2829.

Synthesis of 3

After washing with an appropriate amount of hexane (3×5 mL), NaH (32.7 mg; 60% dispersion in mineral oil, 0.8 mmol) was dissolved in dry DMF (3 mL). This solution was added dropwise in three portions over 15 min to a solution of **2** (133 mg, 0.2 mmol) in DMF (5 mL). During the intervals, a solution of CH_3I (85.2 mg, 0.6 mmol) in DMF (5 mL) was added dropwise. The resulting mixture was stirred for another 2 h. After the reaction was complete as monitored by TLC, dichloromethane (50 mL) was added to the mixture. The resulting organic phase was washed with water (3× 30 mL) and then dried over K_2CO_3. The solvent was removed on a rotary evaporator, and the resulting residue was purified by column chromatography on silica gel (eluent: CH_2Cl_2/ethyl acetate, 25:1) to give **3** (75 mg) as a pale-yellow solid in 54% yield. ^{1}H NMR (400 MHz, [D$_6$]acetone): $\delta=3.11$ (s, 6H), 3.73 (s, 12H), 6.71 (s, 8H), 6.82 (d, $J=8.0$ Hz, 8H), 6.95 ppm (d, $J=8.0$ Hz, 8H); ^{13}C NMR (100 MHz, [D$_6$]DMSO): $\delta=28.45$, 55.15, 114.75, 121.45, 125.28, 126.16, 138.70, 140.59, 144.75, 155.06, 159.83 ppm; MALDI-TOF: *m/z*: 694.4 $[M]^+$; ESI-HRMS: *m/z* calcd for $C_{43}H_{42}N_4O_5$: 694.3155; found: 694.3148.

Synthesis of 5

Following the similar procedure for the synthesis of compound **2**, compound **5** was isolated as a pale-yellow solid from the reaction of compound **4** (123 mg, 0.5 mmol) with triphosgene in 90% yield. ^{1}H NMR (400 MHz, [D$_6$]DMSO): $\delta=7.41$ (t, $J=5.6$ Hz, 4H), 7.94 (t, $J=7.2$ Hz, 4H), 8.06 (d, $J=7.2$ Hz, 4H), 8.37 (s, 4H), 8.73 (s, 4H), 9.86 (s, 2H), 10.21 ppm (s, 2H); ^{13}C NMR (100 MHz, [D$_6$]DMSO): $\delta=$ 116.78, 118.21, 120.46, 122.85, 137.32, 139.76, 140.96, 149.53, 152.99, 155.84 ppm; MALDI-TOF-HRMS: *m/z* calcd for $C_{33}H_{25}N_6O$ $[M+H]^+$: 521.2090; found: 521.2079.

Synthesis of 6$(PF_6)_2$

[(ttpy)RuCl$_3$] (115.0 mg, 0.2 mmol) and AgOTf (180 mg, 0.7 mmol) were added to dry acetone (30 mL). The mixture was heated at reflux for 2 h before cooling to room temperature. The resulting AgCl precipitate was filtered. The filtrate was concentrated, and the residue was dissolved in DMF (15 mL). The solution was then transferred by syringe to a pressure vessel charged with compound **5** (52 mg, 0.1 mmol) in dry *t*BuOH (10 mL). The mixture was bubbled with N_2 for 15 min before the vessel was capped and heated at 120 °C for 12 h. After cooling to room temperature, the reaction mixture was filtered and the solvent was removed under vacuum. To the residue was added methanol (3 mL), followed by the addition of an excess of aq. KPF_6. The resulting precipitate was collected by filtering and washing with water and ethyl ether. This crude product was purified by column chromatography on silica gel (eluent: CH_3CN/H_2O/aq. KNO_3, 100:5:1) to give complex **6**$(PF_6)_2$ as a brown solid in 23% yield. ^{1}H NMR (400 MHz, [D$_6$]acetone): $\delta=$ 2.51 (s, 6H), 6.77 (t, $J=7.0$ Hz, 4H), 7.18 (t, $J=7.0$ Hz, 4H), 7.30 (d, $J=7.0$ Hz, 4H), 7.34 (d, $J=5.2$ Hz, 4H), 7.55 (d, $J=7.6$ Hz, 4H), 7.72 (t, $J=7.6$ Hz, 4H), 7.86 (t, $J=7.6$ Hz, 4H), 8.25 (d, $J=8.4$ Hz, 8H), 8.58 (s, 2H), 8.66 (s, 4H), 8.93 (d, $J=8.0$ Hz, 4H), 9.36 ppm (s, 4H); MALDI-MS: 1512.4 for $[M-PF_6]^+$; elemental analysis calcd (%) for $C_{77}H_{56}F_{12}N_{12}OP_2Ru_2\cdot2H_2O$: C 54.61; H 3.57; N 9.93; found: C 54.45; H 3.35; N 9.94.

Synthesis of 7

Following the similar procedure for the synthesis of compound **3**, compound **7** was isolated as a pale-yellow solid from the reaction of compound **5** (130 mg, 0.25 mmol) in 84% yield. ^{1}H NMR (400 MHz, [D$_6$]DMSO): $\delta=3.30$ (s, 6H), 7.31 (t, $J=5.6$ Hz, 4H), 7.66 (s, 4H), 7.68 (s, 4H), 7.75 (s, $J=7.2$ Hz, 4H), 8.14 (s, 2H), 8.56 ppm (s, 4H); ^{13}C NMR (100 MHz, [D$_6$]DMSO): $\delta=39.36$, 120.28, 120.87, 122.71, 123.97, 136.95, 139.58, 145.80, 149.33, 155.09, 159.23 ppm;

MALDI-TOF-HRMS: *m/z* calcd for $C_{35}H_{29}N_6O$: 549.2403 $[M+H]^+$; found: 549.2396.

Synthesis of 8$(PF_6)_2$

Following the similar procedure for the synthesis of **6**$(PF_6)_2$, complex **8**$(PF_6)_2$ was isolated as a brown solid from the reaction of ligand **7** (54 mg, 0.1 mmol) with 2 equiv of [(ttpy)$RuCl_3$] in 70% yield. ^{1}H NMR (400 MHz, [D$_6$]acetone): $\delta = 2.48$ (s, 6H), 3.67 (s, 6H), 6.02 (s, 4H), 6.73 (s, 4H), 6.91 (s, 4H), 7.24 (s, 4H), 7.53 (d, $J = 7.6$ Hz, 8H), 7.59 (overlapping, 4H), 8.19 (d, $J = 8.0$ Hz, 4H), 8.27 (s, 4H), 8.34 (s, 4H), 8.77 (d, $J = 8.0$ Hz, 4H), 9.29 ppm (s, 4H); MALDI-TOF-MS: *m/z*: 1540.7 $[M-PF_6]^+$; elemental analysis calcd (%) for $C_{79}H_{60}F_{12}N_{12}OP_2Ru_2 \cdot 3H_2O$: C 54.55; H 3.82; N 9.66; found: C 54.52; H 3.76; N 9.39.

Synthesis of 9$(PF_6)_2$

Following the similar procedure for the synthesis of **6**$(PF_6)_2$, complex **9**$(PF_6)_2$ was isolated as a brown solid from the reaction of ligand **7** (33 mg, 0.06 mmol) with 2 equiv of [(Me_3tctpy)$RuCl_3$] in 59% yield. ^{1}H NMR (400 MHz, CD_3CN): $\delta = 3.73$ (s, 6H), 3.76 (s, 12H), 4.15 (s, 6H), 5.96 (d, $J = 4.8$ Hz, 4H), 6.57 (t, $J = 6.4$ Hz, 4H), 6.73 (d, $J = 5.6$ Hz, 4H), 6.89 (d, $J = 5.6$ Hz, 4H), 7.50 (t, $J = 7.6$ Hz, 4H), 8.06 (d, $J = 8.0$ Hz, 4H), 8.18 (s, 4H), 8.80 (s, 4H), 9.35 ppm (s, 4H); MALDI-TOF-MS: *m/z*: 1708.4 $[M-PF_6]^+$; elemental analysis calcd (%) for $C_{79}H_{60}F_{12}N_{12}OP_2Ru_2 \cdot 3H_2O$: C 48.48; H 3.49; N 8.81; found: C 48.41; H 3.29; N 8.85.

Synthesis of 11

A suspension of *N*,*N*-di(*p*-anisyl)-4-iodoaniline (1.01 g, 6.60 mmol), imidazolidin-2-one (4.34 g, 19.8 mmol), CuI (260 mg, 1.40 mmol), and K_2CO_3 (2.84 g, 13.4 mmol) in toluene (25 mL) were stirred for 30 min, followed by the addition of *N*,*N*-dimethylethane-1,2-diamine (226 mL, 204 mg). The system was heated at 120 °C for another 20 h. After cooling to room temperature, the suspension was filtered through Celite and washed with CH_2Cl_2 (2×25 mL). The pale-green filtrate was concentrated to dryness in vacuo and further purified by flash chromatography on silica gel (eluent: CH_2Cl_2/ethyl acetate, 25:1) to give compound **11** (60 mg) as a pale-yellow solid in 43% yield. ^{1}H NMR (400 MHz, [D$_6$]acetone): $\delta = 3.77$ (s, 12H), 4.03 (br, 4H), 6.87 (d, $J = 8.8$ Hz, 8H), 6.93 (d, $J = 9.2$ Hz, 4H), 6.98 (d, $J = 8.8$ Hz, 8H), 7.54 ppm (d, $J = 9.2$ Hz, 4H); ^{13}C NMR (100 MHz, [D$_6$]DMSO): $\delta = 41.65$, 55.19, 114.80, 119.10, 121.91, 125.26, 134.17, 140.80, 143.23, 154.49, 155.02 ppm; MALDI-TOF-MS (*m/z*): 692.5 $[M]^+$; ESI-HRMS: *m/z* calcd for $C_{43}H_{40}N_4O_5$: 692.2999; found: 692.2988.

Synthesis of 12

Following the same procedure for the synthesis of **2**, compound **12** was isolated as a pale-yellow solid from the reaction of N^1,N^1-di(*p*-anisyl)benzene-1,4-diamine (80 mg, 0.25 mmol), triphogene, and *p*-toluidine (29.5 mg, 0.275 mmol) in 71% yield. ^{1}H NMR (400 MHz, [D$_6$]acetone): $\delta = 2.25$ (s, 3H), 3.76 (s, 6H), 6.86 (d, $J = 8.4$ Hz, 6H), 6.96 (d, $J = 7.6$ Hz, 4H), 7.07 (d, $J = 7.6$ Hz, 2H), 7.39 (t, $J = 7.2$ Hz, 4H), 7.97 ppm (s, 2H); ^{13}C NMR (100 MHz, [D$_6$]DMSO): $\delta = 20.30$, 55.19, 114.75, 118.12, 119.55, 122.63, 124.97, 129.11, 130.40, 133.90, 137.23, 141.03, 142.59, 152.60, 154.84 ppm; MALDI-TOF-MS: *m/z*: 453.1 $[M]^+$; ESI-HRMS: *m/z* calcd for $C_{28}H_{27}N_3O_3$: 453.2052; found: 453.2048.

Synthesis of 14

Following the same procedure for the synthesis of **11**, compound **14** was isolated as a pale-yellow solid in 48% yield from the treatment of 2,2′-(5-bromo-1,3-phenylene)dipyridine (155 mg, 0.5 mmol) with 3 equiv of imidazolidin-2-one. ^{1}H NMR (400 MHz, [D$_6$]DMSO): $\delta = 4.22$ (s, 4H), 7.41 (s, 4H), 7.94 (s, 4H), 8.12 (s, 4H), 8.49 (s, 6H), 8.74 ppm (s, 4H); ^{13}C NMR (100 MHz, [D$_6$]DMSO): $\delta = 41.71$, 116.43, 118.98, 120.66, 122.95, 137.35, 139.69, 141.16, 149.54, 154.61, 155.74 ppm; MALDI-TOF-HRMS: *m/z* calcd for $C_{35}H_{27}N_6O$: 547.2246 $[M+H]^+$; found: 547.2240.

Synthesis of 15$(PF_6)_2$

Following the similar procedure for the synthesis of **6**$(PF_6)_2$, complex **15**$(PF_6)_2$ was isolated as a brown solid from the reaction of ligand **14** (33 mg, 0.06 mmol) with 2 equiv of [(ttpy)$RuCl_3$] in 74% yield. ^{1}H NMR (400 MHz, [D$_6$]acetone): $\delta = 2.53$ (s, 6H), 4.65 (s, 4H), 6.81 (t, $J = 6.8$ Hz, 4H), 7.20 (t, $J = 6.8$ Hz, 4H), 7.35 (d, $J = 5.6$ Hz, 8H), 7.57 (d, $J = 8.0$ Hz, 4H), 7.77 (t, $J = 8.0$ Hz, 4H), 7.89 (t, $J = 8.0$ Hz, 4H), 8.26 (d, $J = 8.0$ Hz, 4H), 8.40 (d, $J = 8.0$ Hz, 4H), 8.86 (s, 4H), 8.96 (d, $J = 8.0$ Hz, 4H), 9.40 ppm (s, 4H); MALDI-TOF-MS: *m/z*: 1540.7 $[M-PF_6]^+$; elemental analysis calcd (%) for $C_{79}H_{58}F_{12}N_{12}OP_2Ru_2 \cdot 3H_2O$: C 54.61; H 3.71; N 9.67; found: C 54.64; H 3.59; N 9.64.

Synthesis of 16

Following the similar procedure for the synthesis of **2**, compound **16** was isolated as a pale-yellow solid from the reaction of 3,5-di(-pyridin-2-yl)aniline (124 mg, 0.5 mmol), triphosgene, *p*-toluidine (55 mg, 0.5 mmol) in 88% yield. ^{1}H NMR (400 MHz, [D$_6$]DMSO): $\delta = 2.25$ (s, 3H), 7.11 (d, $J = 8.0$ Hz, 2H), 7.40 (dd, $J = 7.0$, 8.0 Hz, 4H), 7.90–7.95 (overlapping, 2H), 8.03 (d, $J = 8.0$ Hz, 2H), 8.29 (s, 2H), 8.34 (s, 1H), 8.60 (s, 1H), 8.71 (s, 2H), 8.96 ppm (s, 1H); ^{13}C NMR (100 MHz, [D$_6$]DMSO): $\delta = 20.35$, 116.97, 118.24, 118.46, 120.43, 122.85, 129.18, 130.77, 137.04, 137.32, 139.74, 140.86, 149.54, 152.69, 155.81 ppm; MALDI-TOF-HRMS: *m/z* calcd for $C_{24}H_{21}N_4O$: 381.1715 $[M+H]^+$; found: 381.1712.

Synthesis of 17(PF_6)

Following the similar procedure for the synthesis of compound **6**$(PF_6)_2$, complex **17**(PF_6) was isolated as a brown solid from the reaction of compound **16** (33 mg, 0.06 mmol) with 2 equiv of [(ttpy)$RuCl_3$] in 74% yield. ^{1}H NMR (400 MHz, CD_3CN): $\delta = 2.34$ (s, 3H), 2.51 (s, 3H), 6.41 (s, 2H), 6.98 (s, 2H), 7.18–7.43 (overlapping, 10H), 7.34 (d, $J = 8.0$ Hz, 2H), 7.59 (t, $J = 8.0$ Hz, 2H), 7.74 (t, $J = 7.6$ Hz, 2H), 7.83 (s, 2H), 8.11 (d, $J = 8.0$ Hz, 2H), 8.51 (d, $J = 7.6$ Hz, 4H), 9.07 ppm (s, 2H); MALDI-TOF-MS: 804.1 for $[M-PF_6]^+$; elemental analysis calcd (%) for $C_{46}H_{36}F_6N_7OPRu \cdot 2H_2O$: C 56.10; H 4.09; N 9.96; found: C 56.01; H 3.86; N 9.91.

Acknowledgements

We thank the National Natural Science Foundation of China (grants 21472196, 21271176, 91227104, and 21221002), the National Basic Research 973 program of China (grant 2011CB932301), and the Strategic Priority Research Program of the Chinese Academy of Sciences (grant XDB 12010400) for funding support.

Keywords: density functional calculations · mixed-valent compounds · ruthenium · triarylamines · urea

[1] a) V. Coropceanu, J. Cornil, D. A. da Silva Filho, Y. Olivier, R. Silbey, J.-L. Bredas, *Chem. Rev.* **2007**, *107*, 926; b) W. Kaim, G. K. Lahiri, *Angew. Chem.* **2007**, *119*, 1808; *Angew. Chem. Int. Ed.* **2007**, *46*, 1778; c) D. H. Evans, *Chem. Rev.* **2008**, *108*, 2113; d) H. Bässler, A. Köhler, *Top. Curr. Chem.* **2012**, *312*, 1 – 65.

[2] See reviews on mixed-valence chemistry: a) S. F. Nelsen, *Chem. Eur. J.* **2000**, *6*, 581; b) D. M. D'Alessandro, F. R. Keene, *Chem. Rev.* **2006**, *106*, 2270; c) P. Aguirre-Etcheverry, D. O'Hare, *Chem. Rev.* **2010**, *110*, 4839; d) J. Hankache, O. S. Wenger, *Chem. Rev.* **2011**, *111*, 5138; e) S. Heckmann, C. Lambert, *Angew. Chem.* **2012**, *124*, 334; *Angew. Chem. Int. Ed.* **2012**, *51*, 326; f) P. J. Low, N. J. Brown, *J. Cluster Sci.* **2010**, *21*, 235; g) M. H. Chisholm, B. J. Lear, *Chem. Soc. Rev.* **2011**, *40*, 5254; h) A. Hildebrandt, H. Lang, *Organometallics* **2013**, *32*, 5640.

[3] See specific examples on mixed-valence chemistry: a) R. Sakamoto, M. Murata, H. Nishihara, *Angew. Chem.* **2006**, *118*, 4911; *Angew. Chem. Int. Ed.* **2006**, *45*, 4793; b) K. V. Vasudevan, I. Vargas-Baca, A. H. Cowley, *Angew. Chem.* **2009**, *121*, 8519; *Angew. Chem. Int. Ed.* **2009**, *48*, 8369; c) S. D. Glover, C. P. Kubiak, *J. Am. Chem. Soc.* **2011**, *133*, 8721; d) B. Xi, I. P.-C. Liu, G.-L. Xu, M. M. R. Choudhuri, M. C. DeRosa, R. J. Crutchley, T. Ren, *J. Am. Chem. Soc.* **2011**, *133*, 15094; e) M. A. Fox, B. Le Geunnic, R. L. Roberts, D. A. Brue, D. S. Yufit, J. A. K. Howard, G. Manca, J.-F. Halet, F. Hartl, P. J. Low, *J. Am. Chem. Soc.* **2011**, *133*, 18433; f) A. K. Das, B. Sarkar, J. Fiedler, S. Zalis, I. Hartenbach, S. Strobel, G. K. Lahiri, W. Kaim, *J. Am. Chem. Soc.* **2009**, *131*, 8895; g) Y. Li, M. Josowicz, L. M. Tolbert, *J. Am. Chem. Soc.* **2010**, *132*, 10374; h) C. Olivier, K. Costuas, S. Choua, V. Maurel, P. Turek, J.-Y. Saillard, D. Touchard, S. Rigaut, *J. Am. Chem. Soc.* **2010**, *132*, 5638; i) D. Siebler, M. Linseis, T. Gasi, L. M. Carrella, R. F. Winter, C. Forster, K. Heinze, *Chem. Eur. J.* **2011**, *17*, 4540; j) S. Rodríguez Gonzalez, M. C. Ruiz Delgado, R. Caballero, P. De la Cruz, F. Langa, J. T. López Navarrete, J. Casado, *J. Am. Chem. Soc.* **2012**, *134*, 5675; k) M. Linseis, S. Zalis, M. Zabel, R. F. Winter, *J. Am. Chem. Soc.* **2012**, *134*, 16671; l) Y.-P. Ou, J. Zhang, M. Xu, J. Xia, F. Hartl, J. Yin, G.-A. Yu, S. H. Liu, *Chem. Asian J.* **2014**, *9*, 1152; m) Y.-P. Ou, J. Xia, J. Zhang, M. Xu, J. Yin, G.-A. Yu, S. H. Liu, *Chem. Asian J.* **2013**, *8*, 2023; n) X. Xiao, C. Y. Liu, Q. He, M. J. Han, M. Meng, H. Lei, X. Lu, *Inorg. Chem.* **2013**, *52*, 12624; o) K. Kobayashi, M. Ishikubo, K. Kanaizuka, K. Kosuge, S. Masaoka, K. Sakai, K. Nozaki, M.-a. Haga, *Chem. Eur. J.* **2011**, *17*, 6954; p) F. Weisser, R. Huebner, D. Schweinfurht, B. Sarkar, *Chem. Eur. J.* **2011**, *17*, 57277; q) G. E. Pieslinger, P. Albores, L. D. Slep, L. M. Baraldo, *Angew. Chem.* **2014**, *126*, 1317; *Angew. Chem. Int. Ed.* **2014**, *53*, 1293; r) H. S. Das, D. Schweinfurth, J. Fiedler, M. M. Khusniyarov, S. M. Mobin, B. Sakar, *Chem. Eur. J.* **2014**, *20*, 4334.

[4] a) L. L. Miller, K. R. Mann, *Acc. Chem. Res.* **1996**, *29*, 417; b) D.-L. Sun, S. V. Rosokha, S. V. Lindeman, J. K. Kochi, *J. Am. Chem. Soc.* **2003**, *125*, 15950; c) J. Casado, K. Takimiya, T. Otsubo, F. J. Ramirez, J. J. Quirante, R. P. Ortiz, S. R. Gonzalez, M. M. Oliva, J. T. L. Navarrete, *J. Am. Chem. Soc.* **2008**, *130*, 14028; d) D. Cornelis, E. Franz, I. Asselberghs, K. Clays, T. Verbiest, G. Koeckelberghs, *J. Am. Chem. Soc.* **2011**, *133*, 1317; e) S. P. Jagtap, S. Mukhopadhyay, V. Coropceanum, G. L. Brizius, J.-L. Bredas, D. M. Collard, *J. Am. Chem. Soc.* **2012**, *134*, 7176; f) S. T. Schneebeli, M. Frasconi, Z. Liu, Y. Wu, D. M. Gardner, N. L. Strutt, C. Cheng, R. Carmieli, M. R. Wasielewski, J. F. Stoddart, *Angew. Chem.* **2013**, *125*, 13338; *Angew. Chem. Int. Ed.* **2013**, *52*, 13100.

[5] C. Creutz, H. Taube, *J. Am. Chem. Soc.* **1969**, *91*, 3988.

[6] a) I. P.-C. Liu, W.-Z. Wang, S.-M. Peng, *Chem. Commun.* **2009**, 4323; b) R. Sakamoto, S. Katagiri, H. Maeda, H. Nishihara, *Coord. Chem. Rev.* **2013**, *257*, 1493; c) J.-W. Ying, I. P.-C. Liu, B. Xi, Y. Song, C. Campana, J.-L. Zuo, T. Ren, *Angew. Chem.* **2010**, *122*, 966; *Angew. Chem. Int. Ed.* **2010**, *49*, 954; d) J.-P. Launay, *Coord. Chem. Rev.* **2013**, *257*, 1544.

[7] a) N. S. Hush, *Prog. Inorg. Chem.* **1967**, *8*, 391; b) N. S. Hush, *Coord. Chem. Rev.* **1985**, *64*, 135.

[8] N. F. Phelan, M. J. Orchin, *J. Chem. Educ.* **1968**, *45*, 633.

[9] M. Gholami, R. R. Tykwinski, *Chem. Rev.* **2006**, *106*, 4997.

[10] a) M. B. Nielsen, F. Diederich, *Chem. Rev.* **2005**, *105*, 1837; b) H. Hopf, M. S. Sherburn, *Angew. Chem.* **2012**, *124*, 2346; *Angew. Chem. Int. Ed.* **2012**, *51*, 2298; c) W. P. Forrest, Z. Cao, K. M. Hassell, B. M. Prentice, P. E. Fanwick, T. Ren, *Inorg. Chem.* **2012**, *51*, 3261; d) K. B. Vincent, Q. Zeng, M. Parthey, D. S. Yufit, J. A. K. Howard, F. Hartl, M. Kaupp, P. J. Low, *Organometallics* **2013**, *32*, 6022.

[11] H. Hopf, *Angew. Chem.* **1984**, *96*, 947; *Angew. Chem. Int. Ed. Engl.* **1984**, *23*, 948.

[12] C. A. van Walree, B. C. van der Wiel, R. M. Williams, *Phys. Chem. Chem. Phys.* **2013**, *15*, 15234.

[13] A. B. Ricks, G. C. Solomon, M. T. Colvin, A. M. Scott, K. Chen, M. A. Ratner, M. R. Wasielewski, *J. Am. Chem. Soc.* **2010**, *132*, 15427.

[14] D. A. Shultz, R. M. Fico, Jr., S. H. Bodnar, R. K. Kumar, K. E. Vostrikova, J. W. Kampf, P. D. Boyle, *J. Am. Chem. Soc.* **2003**, *125*, 11761.

[15] D. A. Shultz, H. Lee, R. K. Kumar, K. P. Gwaltney, *J. Org. Chem.* **1999**, *64*, 9124.

[16] E. Göransson, R. Emanuelsson, K. Jorner, T. F. Markle, L. Hammarström, H. Ottosson, *Chem. Sci.* **2013**, *4*, 3522.

[17] a) G. C. Solomon, D. Q. Andews, R. H. Goldsmith, T. Hansen, M. R. Wasielewski, R. P. van Duyne, M. A. Ratner, *J. Am. Chem. Soc.* **2008**, *130*, 17301; b) H. Valkenier, C. M. Guedon, T. Markussen, K. S. Thygesen, S. J. van der Molen, J. C. Hummelen, *Phys. Chem. Chem. Phys.* **2014**, *16*, 653.

[18] N. Volz, J. Clayden, *Angew. Chem.* **2011**, *123*, 12354; *Angew. Chem. Int. Ed.* **2011**, *50*, 12148.

[19] a) V. Amendola, L. Fabbrizzi, L. Mosca, *Chem. Soc. Rev.* **2010**, *39*, 3889; b) J. M. Roberts, B. M. Fini, A. A. Sarjeant, O. K. Farha, J. T. Hupp, K. A. Scheidt, *J. Am. Chem. Soc.* **2012**, *134*, 3334; c) L. A. Clare, A. T. Pham, F. Magdaleno, J. Acosta, J. E. Woods, A. L. Cooksy, D. K. Smith, *J. Am. Chem. Soc.* **2013**, *135*, 18930; d) R. Custelcean, *Chem. Commun.* **2013**, *49*, 2173; e) M. Matsumura, A. Tanatani, I. Azumaya, H. Masu, D. Hashizume, H. Kagechika, A. Muranaka, M. Uchiyama, *Chem. Commun.* **2013**, *49*, 2290; f) J. V. Gavette, N. S. Mills, L. N. Zakharov, C. A. Johnson II, D. W. Johnson, M. M. Haley, *Angew. Chem.* **2013**, *125*, 10460; *Angew. Chem. Int. Ed.* **2013**, *52*, 10270; g) C. Luo, K. Tang, Y. Li, D.-L. Yin, X.-G. Chen, H.-H. Huang, *Sci. China Chem.* **2013**, *56*, 1564.

[20] a) K. Yamaguchi, G. Matsumura, H. Kagechika, I. Azumaya, Y. Ito, K. Shudo, *J. Am. Chem. Soc.* **1991**, *113*, 5474; b) T. L. Kurth, F. D. Lewis, *J. Am. Chem. Soc.* **2003**, *125*, 13760; c) J. Clayden, L. Lemiegre, G. A. Morris, M. Pickworth, T. J. Snape, L. H. Jones, *J. Am. Chem. Soc.* **2008**, *130*, 15193; d) S. Hisamatsu, H. Masu, I. Azumaya, M. Takahashi, K. Kishikawa, S. Kohmoto, *Cryst. Growth Des.* **2011**, *11*, 5387; e) F. D. Lewis, T. L. Kurth, C. M. Hattan, R. C. Reiter, C. D. Stevenson, *Org. Lett.* **2004**, *6*, 1605; f) J. Clayden, M. Pickworth, L. H. Jones, *Chem. Commun.* **2009**, 547; g) J. Clayden, L. Lemiegre, M. Pickworth, L. Jones, *Org. Biomol. Chem.* **2008**, *6*, 2908; h) J. Clayden, U. Hennecke, M. A. Vincent, I. H. Hillier, M. Helliwell, *Phys. Chem. Chem. Phys.* **2010**, *12*, 15056.

[21] a) F. D. Lewis, P. Daublain, G. B. D. Santos, W. Liu, A. M. Asatryan, S. A. Markaria, T. Fiebig, M. Raytchev, Q. Wang, *J. Am. Chem. Soc.* **2006**, *128*, 4792; b) T. A. Zeidan, Q. Wang, T. Fiebig, F. D. Lewis, *J. Am. Chem. Soc.* **2007**, *129*, 9848.

[22] A. El-Kasmi, D. Lexa, P. Maillard, M. Momenteau, J.-M. Saveant, *J. Phys. Chem.* **1993**, *97*, 6090.

[23] a) C. Lambert, G. Nöll, *J. Am. Chem. Soc.* **1999**, *121*, 8434; b) C. Lambert, G. Nöll, J. Schelter, *Nat. Mater.* **2002**, *1*, 69; c) A. V. Szeghalmi, M. Erdmann, V. Engel, M. Schmitt, S. Amthor, V. Kriegisch, G. Nöll, R. Stahl, C. Lambert, D. Leusser, D. Stalke, M. Zabel, J. Popp, *J. Am. Chem. Soc.* **2004**, *126*, 7834; d) S. C. Jones, V. Coropceanu, S. Barlow, T. Kinnibrugh, T. Timofeeva, J.-L. Brédas, S. R. Marder, *J. Am. Chem. Soc.* **2004**, *126*, 11782; e) S. Barlow, C. Risko, S.-J. Chung, N. M. Tucker, V. Coropceanu, S. C. Jones, Z. Levi, J.-L. Brédas, S. R. Marder, *J. Am. Chem. Soc.* **2005**, *127*, 16900; f) A. Heckmann, S. Amothor, C. Lambert, *Chem. Commun.* **2006**, 2959; g) S. Barlow, C. Risko, V. Coropceanu, N. M. Tucker, S. C. Jones, Z. Levi, V. N. Khrustalev, M. Y. Antipin, T. L. Kinniburgh, T. Timofeeva, S. R. Marder, J.-L. Brédas, *Chem. Commun.* **2005**, 764; h) J. C. Lacroix, K. I. Chane-Ching, F. Maquere, F. Maurel, *J. Am. Chem. Soc.* **2006**, *128*, 7264; i) G. Zhou, M. Baumgarten, K. Müllen, *J. Am. Chem. Soc.* **2007**, *129*, 12211; j) R. Sakamoto, T. Sasaki, N. Honda, T. Yamamura, *Chem. Commun.* **2009**, 5156; k) S. F. Völker, M. Renz, M. Kaupp, C. Lambert, *Chem. Eur. J.* **2011**, *17*, 14147; l) B. He, O. S. Wenger, *J. Am. Chem. Soc.* **2011**, *133*, 17027; m) S. Barlow, C. Risko, S. A. Odom, S. Zheng, V. Coropceanu, L. Beverina, J.-L. Bredas, S. R. Marder, *J. Am. Chem. Soc.* **2012**, *134*, 10146; n) H.-J. Nie, X. Chen, C.-J. Yao, Y.-W. Zhong, G. R. Hutchison, J. Yao, *Chem. Eur. J.* **2012**, *18*, 14497; o) C.-J. Yao, R.-H. Zheng, H.-J. Nie, B.-B. Cui, Q. Shi, J. Yao, Y.-W. Zhong, *Chem. Eur. J.* **2013**, *19*, 12376; p) M.

Parthey, K. B. Vincent, M. Renz, P. A. Schauer, D. S. Yuft, J. A. K. Howard, M. Kaupp, P. J. Low, *Inorg. Chem.* **2014**, *53*, 1544.

[24] a) J.-P. Sutter, D. M. Grove, M. Beley, J.-P. Collin, N. Veldman, A. L. Spek, J.-P. Sauvage, G. van Koten, *Angew. Chem.* **1994**, *106*, 1359; *Angew. Chem. Int. Ed. Engl.* **1994**, *33*, 1282; b) P. Steenwinkel, D. M. Grove, N. Veldman, A. L. Spek, G. van Koten, *Organometallics* **1998**, *17*, 5647; c) C. Patoux, J.-P. Launay, M. Beley, S. Chodorowski-Kimmers, J.-P. Collin, S. James, J.-P. Sauvage, *J. Am. Chem. Soc.* **1998**, *120*, 3717; d) M. Gagliardo, C. H. M. Amijs, M. Lutz, A. L. Spek, R. W. A. Havenith, F. Hartl, G. P. M. van Klink, G. van Koten, *Inorg. Chem.* **2007**, *46*, 11133; e) S. H. Wadman, R. W. A. Havenith, M. Lutz, A. L. Spek, G. P. M. van Klink, G. van Koten, *J. Am. Chem. Soc.* **2010**, *132*, 1914; f) C.-J. Yao, Y.-W. Zhong, J. Yao, *J. Am. Chem. Soc.* **2011**, *133*, 15697; g) J.-Y. Shao, Y.-W. Zhong, *Chem. Eur. J.* **2014**, *20*, 8702.

[25] C.-W. Chang, G.-S. Liou, *J. Mater. Chem.* **2008**, *18*, 5638.

[26] Z.-L. Gong, Y.-W. Zhong, *Organometallics* **2013**, *32*, 7495.

[27] M. N. Patel, D. S. Gandhi, P. A. Parmar, *Spectrochim. Acta Part A* **2011**, *84*, 243.

[28] J.-Y. Shao, W.-W. Yang, J. Yao, Y.-W. Zhong, *Inorg. Chem.* **2012**, *51*, 4343.

[29] J.-L. Song, P. Amaladass, S.-H. Wen, K. K. Pasunooti, A. Li, Y.-L. Yu, X. Wang, W.-Q. Deng, X.-W. Liu, *New J. Chem.* **2011**, *35*, 127.

[30] C.-J. Yao, R.-H. Zheng, Q. Shi, Y.-W. Zhong, J. Yao, *Chem. Commun.* **2012**, *48*, 5680.

[31] a) W. E. Geiger, F. Barrière, *Acc. Chem. Res.* **2010**, *43*, 1030; b) R. LeSuer, C. Bettolph„ W. E. Geiger, *Anal. Chem.* **2004**, *76*, 6395; c) D. M. D'Alessandro, F. R. Keene, *Dalton Trans.* **2004**, 3950.

[32] a) M. Matis, P. Rapta, V. Lukeš, H. Hartmann, L. Dunsch, *J. Phys. Chem. B* **2010**, *114*, 4451; b) R. Reynolds, L. L. Line, R. F. Nelson, *J. Am. Chem. Soc.* **1974**, *96*, 1087; c) K. Sreenath, T. G. Thomas, K. R. Gopidas, *Org. Lett.* **2011**, *13*, 1134.

[33] W.-W. Yang, Y.-W. Zhong, S. Yoshikawa, J.-Y. Shao, S. Masaoka, K. Sakai, J. Yao, M.-a. Haga, *Inorg. Chem.* **2012**, *51*, 890.

[34] M. B. Robin, P. Day, *Adv. Inorg. Chem. Radiochem.* **1968**, *10*, 247.

[35] C. Lambert, G. Noll, *Angew. Chem.* **1998**, *110*, 2239; *Angew. Chem. Int. Ed.* **1998**, *37*, 2107.

[36] S. Fraysse, C. Coudret, J.-P. Launay, *J. Am. Chem. Soc.* **2003**, *125*, 5880.

[37] a) E. Fukuzaki, H. Nishide, *J. Am. Chem. Soc.* **2006**, *128*, 996; b) Y. Yokoyama, D. Sakanaki, A. Ito, K. Tanaka, M. Shiro, *Angew. Chem.* **2012**, *124*, 9537; *Angew. Chem. Int. Ed.* **2012**, *51*, 9403; c) D. Sakamaki, A. Ito, K. Furukawa, T. Kato, M. Shiro, K. Tanaka, *Angew. Chem.* **2012**, *124*, 12948; *Angew. Chem. Int. Ed.* **2012**, *51*, 12776; d) Z. Ning, H. Tian, *Chem. Commun.* **2009**, 5483; e) P. Bujak, I. Kulszewicz-Bajer, M. Zagorska, V. Maurel, I. Wielgus, A. Pron, *Chem. Soc. Rev.* **2013**, *42*, 8895.

[38] M. Abe, *Chem. Rev.* **2013**, *113*, 7011.

[39] S. Patra, B. Sarkar, S. M. Mobin, W. Kaim, G. K. Lahiri, *Inorg. Chem.* **2003**, *42*, 6469.

[40] Gaussian 09, Revision A.2, M. J. Frisch, G. W. Trucks, H. B. Schlegel, G. E. Scuseria, M. A. Robb, J. R. Cheeseman, J. A. Montgomery, T. Vreven Jr., K. N. Kudin, J. C. Burant, J. M. Millam, S. S. Iyengar, J. Tomasi, V. Barone, B. Mennucci, M. Cossi, G. Scalmani, N. Rega, G. A. Petersson, H. Nakatsuji, M. Hada, M. Ehara, K. Toyota, R. Fukuda, J. Hasegawa, M. Ishida, T. Nakajima, Y. Honda, O. Kitao, H. Nakai, M. Klene, X. Li, J. E. Knox, H. P. Hratchian, J. B. Cross, C. Adamo, J. Jaramillo, R. Gomperts, R. E. Stratmann, O. Yazyev, A. J. Austin, R. Cammi, C. Pomelli, J. W. Ochterski, P. Y. Ayala, K. Morokuma, G. A. Voth, P. Salvador, J. J. Dannenberg, V. G. Zakrzewski, S. Dapprich, A. D. Daniels, M. C. Strain, O. Farkas, D. K. Malick, A. D. Rabuck, K. Raghavachari, J. B. Foresman, J. V. Ortiz, Q. Cui, A. G. Baboul, S. Clifford, J. Cioslowski, B. B. Stefanov, G. Liu, A. Liashenko, P. Piskorz, I. Komaromi, R. L. Martin, D. J. Fox, T. Keith, M. A. Al-Laham, C. Y. Peng, A. Nanayakkara, M. Challacombe, P. M. W. Gill, B. Johnson, W. Chen, M. W. Wong, C. Gonzalez, J. A. Pople, Gaussian, Inc., Wallingford CT, **2009**.

[41] a) A. D. Becke, *J. Chem. Phys.* **1993**, *98*, 5648; b) C. Lee, W. Yang, R. G. Parr, *Phys. Rev. B* **1988**, *37*, 785.

[42] a) P. J. Hay, W. R. Wadt, *J. Chem. Phys.* **1985**, *82*, 270; b) P. J. Hay, W. R. Wadt, *J. Chem. Phys.* **1985**, *82*, 299.

[43] T. H. Dunning, P. J. Hay, in *Modern Theoretical Chemistry, Vol. 3* (Ed.: H. F. Schaefer), Plenum, New York, **1976**, p. 1.

[44] a) M. Renz, K. Theilacker, C. Lambert, M. Kaupp, *J. Am. Chem. Soc.* **2009**, *131*, 16292; b) M. Kaupp, M. Renz, M. Parthey, M. Stolte, F. Würthner, C. Lambert, *Phys. Chem. Chem. Phys.* **2011**, *13*, 16973.

[45] S. B. Nielsen, M. B. Nielsen, A. Rubio, *Acc. Chem. Res.* **2014**, *47*, 1417.

[46] G. M. Sheldrick, *Acta Crystallogr. Sect. A* **2008**, *64*, 112.

[47] O. V. Dolomanov, L. J. Bourhis, R. J. Gildea, J. A. K. Howard, H. Puschmann, *J. Appl. Crystallogr.* **2009**, *42*, 339.

Received: September 18, 2014
Published online on November 24, 2014

